Ideally ordered 10 nm channel arrays grown by anodization of focused-ion-beam patterned aluminum

C. Y. Peng
Physics Department, National Taiwan University, Taipei, Taiwan and Institute of Atomic and Molecular Sciences, Academia Sinica, P. O. Box 23-166, Taipei 106, Taiwan

C. Y. Liu
Institute of Atomic and Molecular Sciences, Academia Sinica, P. O. Box 23-166, Taipei 106, Taiwan

N. W. Liu
Institute of Atomic and Molecular Sciences, Academia Sinica, P. O. Box 23-166, Taipei 106, Taiwan and Materials Science and Engineering Department, National Taiwan University, Taipei, Taiwan

H. H. Wang
Physics Department, National Taiwan University, Taipei, Taiwan and Institute of Atomic and Molecular Sciences, Academia Sinica, P. O. Box 23-166, Taipei 106, Taiwan

A. Datta[a)]
Institute of Atomic and Molecular Sciences, Academia Sinica, P. O. Box 23-166, Taipei 106, Taiwan

Y. L. Wang[b)]
Physics Department, National Taiwan University, Taipei, Taiwan and Institute of Atomic and Molecular Sciences, Academia Sinica, P. O. Box 23-166, Taipei 106, Taiwan

(Received 20 October 2004; accepted 7 February 2005; published 23 March 2005)

Arrays of ideally ordered alumina nanochannels with unprecedented ~10 nm pore size, 40–50 nm interpore spacing, and improved channel uniformity have been fabricated by anodizing an aluminum substrate with a guiding pattern on its surface. The pattern is an array of hexagonally close-packed concaves fabricated by focused ion beam direct sputtering; and its lattice constant is carefully matched to the conditions of the subsequent anodization process in order to achieve effective guiding in the growth of the nanochannels and therefore the ordering of an array. © *2005 American Vacuum Society.* [DOI: 10.1116/1.1884123]

Porous anodic aluminum oxide (AAO) films have been exploited as templates for the growth of nanomaterials with special magnetic,[1] electronic, and/or optical properties[2] because the pores formed spontaneously during anodization are straight and parallel channels on the nanometer scale. For example, AAO films with different average interpore spacing (S) and pore diameter (D) were used to grow carbon nanotubes[3] and metals such as Cu and Ni.[4,5] To fully explore the potential quantum properties of these nanomaterials, it is desirable to further reduce the size and improve the uniformity as well as order of the nanochannels.[6] The current status of the growth technology for the AAO nanochannel array is that, using certain electrolyte solutions and corresponding anodization voltages, the nanochannels can self-organize into hexagonally close-packed (HCP) domains with an average size of a few micrometers.[7,8] For example, using 0.3 M oxalic acid and an anodization voltage of 40 V, the best self-organized order was achieved on arrays with $S=100$ nm. Although the nanochannels of such self-organized arrays also exhibit improved size uniformity, the presence of irregular channels on the domain boundaries sets a severe limitation on its further improvement. Therefore, increasing the domain size is not only an important challenge by itself but also an essential measure for improving the size uniformity of nanochannel arrays on AAO films.

To date, four approaches have been developed to fabricate ideally ordered nanochannel arrays (Some researchers prefer to use the term "single-domain" or "long-range ordered" rather than "ideally ordered" to describe an array grown with the help of some guiding techniques.) On AAO film: imprint lithography with a SiC-mold,[9,10] direct focused ion beam (FIB) lithography,[11] holographic lithography,[12] and resist-assisted FIB lithography.[13] These lithographic methods first create an ordered array of concaves on the Al surface and then use these concaves as "pinning points" to fix the positions of the nanochannels and therefore eliminate the misalignment between different domains of nanochannels formed in a self-organized channel formation process. Although the mechanism of pinning remains an issue to be clarified and may well be slightly different for different lithographic guiding method, it relies most likely on the fact that the oxide growth front in the bottom of the concaves are deeper than that formed spontaneously on the flat area during the initial phase of oxidation. Such head start in the oxide growth front allows the lateral positions of nanochannels to be pinned down on the centers of the concaves. To date, the imprint-lithography guiding method has produced ideally ordered nanochannel arrays with the smallest S of 63 nm.[10] To

a)Present address: Department of Physics, Netaji Nagar Day College, 170/436 N.S.C. Bose Road, Regent Estate, Kolkata 700092.
b)Author to whom correspondence should be addressed; electronic mail: ylwang@pub.iams.sinica.edu.tw

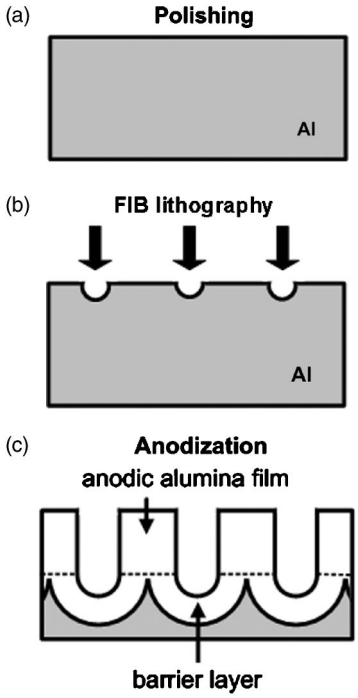

FIG. 1. Schematic diagram showing the process for fabricating anodic alumina film with ideally ordered nanochannels.

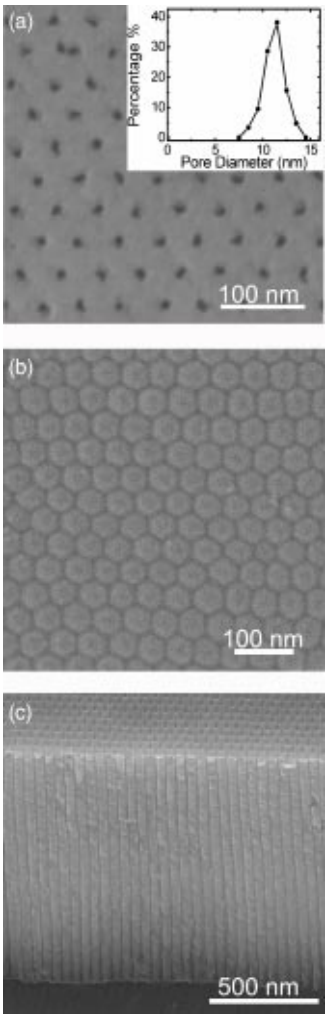

FIG. 2. SEM images of a typical ideally ordered nanochannel array with lattice constant of 50 nm, (a) top view, and (b) bottom view. The inset in (a) shows the corresponding pore size distribution; and (c) cross sectional view of the array demonstrating its aspect ratio of ~100.

further explore the potential applications of such AAO film with ideally ordered array of nanochannels as templates for high-density memories, quantum devices, and novel nanocomposites, it is desirable to further reduce the S of an array. In this paper, we report the achievement of ideally ordered nanochannel arrays with unprecedented S of 40–50 nm and D in the 10 nm range by using a FIB-lithography guided growth method.

As shown schematically in Fig. 1, the fabrication process starts from electropolishing a piece of high purity (99.99%) annealed Al foil (thickness of ~200 μm) in a mixture of 50% $HClO_4$ and C_2H_5OH (volume ratio 1:5) under a constant voltage of 5 V. After polishing, the root-mean-square surface roughness of the sample is typical 1 nm on a 10 $\times 10$ μm^2 area, as measured by a contact mode atomic force microscope (AFM) in air. A 50 keV Ga FIB with a beam diameter of ~10 nm and current of 1.1 pA is then employed to create ordered HCP arrays of 3 nm deep concaves on the Al surface. The patterned sample is anodized in 0.3 M sulfuric acid at 5 °C for 5 min using an anodization voltage that is derived from the empirical relationship: $S = 2.5$ nm per volt.[9] When needed, the surface morphology of anodized samples is inspected by a scanning electron microscope (SEM) with beam energy and diameter of 15 keV and ~3 nm, respectively.

To quantify the dimensions of the nanochannels, we adopt the following procedure to measure the pore size of a nanochannel from its SEM image derived from secondary electron signals. First, the total cross sectional area (A) of a pore is defined as the region within a closed curve whose secondary electron intensity is mid-way between the minimum (pore center) and maximum (far away from the pore). Since the curve is not an exact circle usually, the nominal pore size is then defined as $D_n \equiv (4A/\pi)^{1/2}$. The size uniformity of the pores is expressed by the ratio $\Delta D_n / \langle D_n \rangle$, where ΔD_n and $\langle D_n \rangle$ are the standard deviation and average of the nominal pore size, respectively.

Provided the guiding process is effective, the S of an array can be selected in principle by setting the S of the HCP guiding pattern. Figure 2(a) shows the top view SEM image of a guided nanochannel array with $S = 50$ nm, while its inset plots the size distribution of the pores before post-anodization etching treatment. The distribution peaks at 11–12 nm while $\langle D_n \rangle$ and ΔD_n are 11 nm and 1 nm, respectively. The small pore size and very narrow size distribution, as compared to that of the unguided nanochannels (not shown), clearly demonstrate the merits of guided growth by FIB-lithographic patterning. Figures 2(b) and 2(c) show the bottom and cross-sectional view of the array respectively. These images indicate that the nanochannels with an aspect ratio (length/D_n) of ~100 remain straight and parallel across

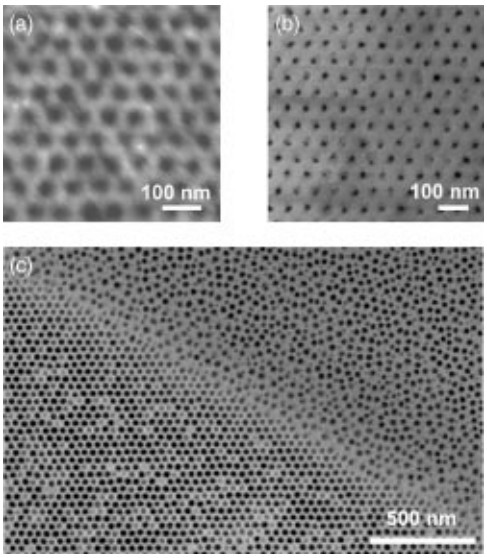

FIG. 3. (a) AFM image of an HCP array of concaves (lattice constant =40 nm) created by FIB on an aluminum surface. Top-view SEM image of (b) an area with guiding pattern after 5 min of anodization, (c) a boundary area between unguided (upper right) and guided (lower left) nanochannels after etching treatment.

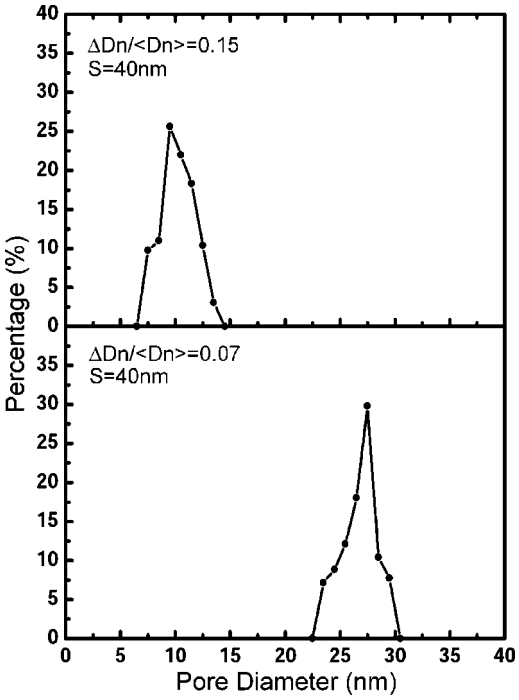

FIG. 4. Pore size distribution of ideally ordered nanochannel arrays with channel spacing 40 nm (a) before and (b) after etching treatment.

the entire AAO film of 1 μm thick. Such a high aspect ratio ideally ordered nanochannel array with $S=50$ nm is already a very attractive template for the growth of ordered array of one-dimensional nanowires and nanocomposites. Closed up view (not shown) of Fig. 2(c) indicates that the sizes of the pores open only slightly (<10%) in the initial (few tens nanometers) growth of the AAO film, further confirming the uniformity of the nanochannels along the growth direction.

Figure 3(a) shows an AFM image of a typical array of concaves created on an Al surface by FIB lithography. The S of the guiding lattice is 40 nm and concaves are 3 nm deep (ion dose of 10^{16} ions/cm^2). After anodization, the top view SEM image of the sample [Fig. 3(b)] shows a similar structure as Fig. 3(a), which clearly demonstrates that the shallow concaves act as effective pinning points to fix the lateral positions of nanochannels in the anodization process even at this unprecedented small S of 40 nm. To further illustrate the precision in the order and uniformity of the array, Fig. 3(c) shows a large scale SEM image of a boundary between guided and unguided nanochannels after the sample is etched in a 5% phosphoric acid for 5 min to open the pores. The apparent morphological difference between the guided (lower left) and unguided (upper right) region clearly shows the guided growth improves not only the order of an array but also its size uniformity.

Figure 4(a) plots the distribution of D_n of the nanochannel array with $S=40$ nm, indicating that the $\langle D_n\rangle$ and ΔD_n of these nanochannels with an aspect ratio of 20 are 10 nm and 1.5 nm, respectively, both of which are rather close to that of the array with $S=50$ nm (Fig. 2). The results clearly indicate that, as S is further reduced from the unprecedented low values of 50 nm to 40 nm, there is a reduction in the $\langle D_n\rangle$ of such ordered nanochannel arrays. However, the ΔD_n appears to increase with the reduction of S. Such a somewhat larger nanochannel uniformity, $\Delta D_n/\langle D_n\rangle$, can be reduced from 0.15 to 0.07 by etching the array in a 5% phosphoric acid for 5 min [Fig. 4(b)], but the improvement is at the expense of increasing $\langle D_n\rangle$ from 10 to 27 nm. In other words, chemical etching does not decrease ΔD_n. The apparent improvement in the uniformity of guided nanochannels shown in Fig. 3(c) is only relative rather than absolute.

To push the limit in the smallest size of the nanohannels that can be fabricated by the FIB-lithography guided growth method, a sample with a guiding lattice of $S=30$ nm was anodized at 12 V for 5 min. Figure 5(a) shows the top view image of an AAO film at the boundary of the FIB-patterned area. The image demonstrates that the right side (patterned region) is ordered while the left side (unguided region) is irregular, and the guided growth method remains effective initially even at such a small scale. Figure 5(b) shows the barrier layer structure of the patterned region of Fig. 5(a). The array appears to maintain a good degree of orientational order, as supported by the six well-defined peaks in the two-dimensional Fourier transform of the image [inset of Fig. 5(b)]. However, local distortion in the order of the array can be clearly observed in Fig. 5(b). For comparison, Fig. 5(c) shows the barrier layer of the array in the unguided region. The complete loss of orientational order in the unguided arrays is clearly demonstrated by ringlike structure in the two-dimensional Fourier transform [inset of Fig. 5(c)] of the image. The results of this effort suggest that, although the guiding lattice does not entirely dominate the growth of

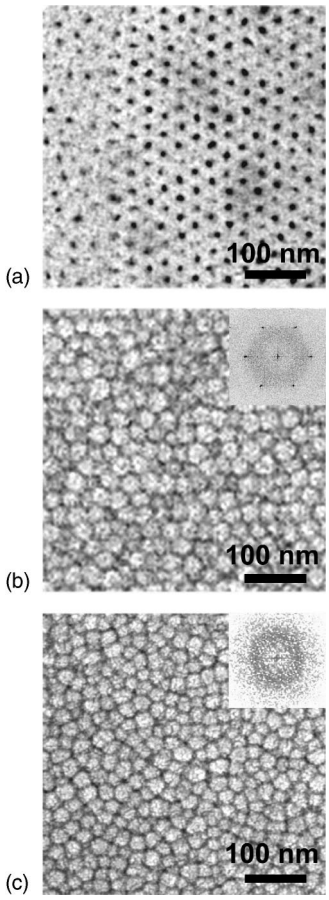

FIG. 5. SEM images of a nanochannel array grown by anodizing an aluminum with a guiding lattice of $S=30$ nm on its surface (a) top view of a boundary between unguided and guided region. (b) and (c) show the barrier layer of guided and unguided region, respectively. The insets in (b) and (c) show the corresponding two-dimensional Fourier transform of the images.

nanochannels at such a small S, the order of a guided array still shows significant improvement over that of an unguided array.

The imperfect guiding by the FIB-patterning in the growth of an array with $S=30$ nm can be partly understood in terms of the observations found in our previous study of the order–disorder transition in the growth of arrays with S of ~ 100 nm.[14] The observations indicate that the HCP guiding pattern must have a lattice constant very close to the S determined by the anodization voltage. Furthermore, for a given acid electrolyte, the anodization voltage must lie with certain range in order to grow a self-organized HCP array with domains of few microns in size. Based on these observations, the concept of "lattice matching" has been adopted to describe the adequacy of the guiding lattice. For an array grown under the guidance of a precisely matched guiding pattern, the length of the nanochannels is practically unlimited, while finite lattice mismatch leads to the existence of a critical channel length, beyond which defects appear on an initially ordered array. Therefore, the loss of effective guiding is due primarily to the use of sulfuric acid for the anodization in 12 V. The combination does not create a self-organization mechanism and therefore the effect of guiding pattern diminishes very quickly as the channels grow. A possible secondary cause of the imperfection in the guiding can be attributed to the reduction in the relative accuracy of the guiding pattern as its S is reduced. Since the FIB has finite beam diameter of ~ 10 nm, the corresponding uncertainty in the positions of each guiding concave may not be negligible when S approaches 30 nm. The primary cause is intrinsic and can only be overcome by the use of another electrolyte that is yet to be found, while the secondary cause is extrinsic and can be solved by the use a better focused FIB.

In summary, we have successfully fabricated ideally ordered HCP arrays of nanochannels on AAO film with unprecedented small pore size of ~ 10 nm and lattice constant between 40–50 nm. Focused ion beam lithography is used to pattern a highly ordered array of shallow concaves on an electro-polished Al sample surface, which act as pinning points for guiding the channel-growth in the latter anodization process. The uniformity in the size of the ideally ordered nanochannels shows significant improvement. The attempt to fabricate an ideally ordered array with an even smaller S of 30 nm is only partially successful primarily because of the lack of an acid that can produce a self-organized array with $S=30$ nm. The success in the fabrication of ideally ordered array of nanochannels with such unprecedented small pore size and separation could open up many novel potential applications of this unique porous AAO template. For example, arrays with small pore size could be exploited for applications that rely on the properties derived from the confinement effect of material inside individual nanochannels; while arrays with small pore separation might be used to take advantage of the collective interference effect originated from proximity effect between neighboring nanochannels.

This work was partly funded by the National Science Council (NSC-93-2120-M-001-002) of Taiwan. C. Y. Liu acknowledges the fellowship provided by Academia Sinica, Taiwan.

[1]P. Aranda and J. M. Garcia, J. Magn. Magn. Mater. **249**, 214 (2002).
[2]H. Masuda, M. Ohya, K. Nishio, H. Asoh, M. Nakao, M. Nohtomi, A. Yokoo, and T. Tamamura, Jpn. J. Appl. Phys., Part 2 **39**, L1039 (2000).
[3]J. Li, C. Papadopoulos, and J. M. Xu, Appl. Phys. Lett. **75**, 367 (1999).
[4]Q. F. Zhan, Z. Y. Chen, D. S. Xue, F. S. Li, H. Kunkel, X. Z. Zhou, R. Roshko, and G. Williams, Phys. Rev. B **66**, 134436 (2002).
[5]S. Melle, J. L. Menendez, G. Armelles, D. Navas, M. Vazquez, K. Nielsch, R. B. Wehrspohn, and U. Gösele, Appl. Phys. Lett. **83**, 4547 (2003).
[6]N. Kouklin, L. Menon, and S. Bandyopahyay, Appl. Phys. Lett. **80**, 1649 (2002).
[7]F. Li, L. Zhang, and R. M. Metzger, Chem. Mater. **10**, 2470 (1998).
[8]A. P. Li, F. Müller, A. Birner, K. Nielsch, and U. Gösele, J. Appl. Phys. **84**, 6023 (1998).
[9]H. Masuda, H. Yamada, M. Satoh, and H. Asoh, Appl. Phys. Lett. **71**, 2770 (1997).
[10]H. Asoh, K. Nishio, M. Nakao, A. Yokoo, T. Tamamura, and H. Masuda, J. Vac. Sci. Technol. B **19**, 569 (2001).
[11]C. Y. Liu, A. Datta, and Y. L. Wang, Appl. Phys. Lett. **78**, 120 (2001).
[12]Z. Sun and H. K. Kim, Appl. Phys. Lett. **81**, 3458 (2002).
[13]N. W. Liu, A. Datta, C. Y. Liu, and Y. L. Wang, Appl. Phys. Lett. **82**, 1281 (2003).
[14]C. Y. Liu, A. Datta, N. W. Liu, C. Y. Peng, and Y. L. Wang, Appl. Phys. Lett. **84**, 2509 (2004).